Seismic performance of single-storey steel CBF structures constructed in the 1960s

A. Caruso-Juliano[1], A. Gallagher[1], T.E. Morrison[2], C.A. Rogers[3]

[1] SDK et associés, Montreal, Canada

[2] Heritage Standing Inc., Fredericton, Canada

[3] Dept. of Civil Engineering and Applied Mechanics, McGill University, Montreal, Canada

[3]Corresponding author

Tel. 514 398-6449

Fax.514 398-7361

colin.rogers@mcgill.ca

Dept. of Civil Engineering and Applied Mechanics

McGill University

Macdonald Engineering Building

817 Sherbrooke Street West

Montreal, QC, Canada, H3A 0C3

Abstract

A general overview of the seismic performance of representative single-storey CBF buildings designed using the 1965 National Building Code of Canada and the 1965 S16 Canadian Standards Association Steel Structures for Buildings Standard was obtained through the use of non-linear time history dynamic analyses and the testing of brace elements obtained from buildings constructed in the 1960s. The study comprised 16 representative buildings subjected to 20 site selected ground motions for three locations; Halifax (Nova Scotia) low seismicity, Montreal (Quebec) moderate seismicity, and Abbotsford (British Columbia) high seismicity. Incremental dynamic analyses were performed using various failure criteria as obtained from the test data; brace net-section fracture, bolt shear, block shear, bolt bearing and brace yielding. Fragility curves were created and the probability of failure was defined. The performance of the structures designed for Abbotsford was unsatisfactory for all of the brace connection failure mechanisms. In contrast, because of the lower current seismic hazard in Montreal, the 16 archetypical buildings demonstrated better performance. In Halifax the buildings performed well, based on the identified failure criteria. It was necessary to strengthen the roof diaphragms for all buildings to carry 2010 NBCC design level seismic forces.

Keywords: Steel; single-storey building; braced frame; existing structures; seismic; performance; analyses

1 INTRODUCTION

1.1 Background

Concern exists regarding the significant portion of Canadian infrastructure that was designed and built prior to the beginnings of modern seismic structural engineering design provisions first developed in the 1970s. Substantial updates to the Canadian design codes and standards have since been implemented (Mitchell et al. 2010); this has resulted in the potential for steel buildings designed and constructed in the 1960s to not meet current seismic performance expectations. Existing structures may require attention in terms of seismic evaluation and possible retrofit.

Concentrically braced frame (CBF) structures are defined in the CSA S16-2009 Design of Steel Structures Standard as "those in which the centre-lines of diagonal braces, beams and columns are approximately concurrent with little or no joint eccentricity" (CSA 2009). Single-storey CBF buildings rely on the diagonal braces in the walls and the steel deck roof diaphragm to transfer lateral wind and seismic loads through to the foundation (Figure 1). With the introduction of seismic requirements in the building codes of the 1960s CBFs were frequently chosen over moment resisting frames as drift became an important design consideration (Bruneau et al. 1998). CBFs employ high elastic lateral stiffness and resist lateral loads based on axial action of the braces, with very little bending or flexural action. The initial design philosophy of codes of the 1960s for wind loads was that braces were to remain in the linear elastic range. At the time, this principle was also applied for seismic design; as such, buildings were not detailed for inelastic seismic response (Figure 2a). Later codes recognised the cyclic inelastic behaviour of CBFs that led to the introduction of the capacity design procedures and detailing (Figure 2b) that are an integral component of modern steel seismic design provisions (Bruneau et al. 1998).

The current seismic design philosophy according to the 2010 National Building Code of Canada (NBCC) (NRCC 2010) and CSA S16 (2009) incorporates the principle of capacity design for most structural steel lateral load carrying systems. A specific element in the lateral force resisting system is designed to dissipate energy through inelastic response under seismic loads. The other elements of the lateral framing system are designed such that they have adequate resistance, while remaining

elastic, so that the fuse element can dissipate the required energy (Figure 2b). This ensures a hierarchy for yielding such that the inelastic response is constrained to the specified element. In CBFs defined by CSA S16-2009 as either having moderate ductility (MD) or limited ductility (LD) the element designed to dissipate energy and withstand the large deformations anticipated under the design level earthquake is the brace, which provides ductility by means of tension yielding along its length and compression buckling. The NBCC prescribes that the building be able to undergo such deformations while remaining intact to enable evacuation, preventing major failure and loss of life.

1.2 Objectives and scope of study

The central objective of the research described in this paper was to obtain a general overview of the seismic performance of existing single-storey steel CBF buildings designed and constructed in Canada during the 1960s, where the braces were selected using the principle that they remain within the linear elastic stress range (Figure 2a) (Caruso-Juliano 2012, Gallagher 2012). The scope of study involved the design of 16 uniquely dimensioned buildings using the 1965 NBCC (NRCC 1965) and CSA S16-1965 (1965) steel standard for each of the following cities; Halifax, NS, Montreal, QC, and Abbotsford, BC. Analysis and design assumptions were similar to those made by practicing engineers within the focus time period. The structural analysis software OpenSees (McKenna 1997, Mazzoni et al. 2009) was utilized to numerically model each building and to capture the inelastic brace and brace connection behaviour of the structures when subjected to ground motions representing the current earthquake hazard prescribed in the 2010 NBCC. Testing of braces obtained from an existing structure built in the 1960s and an additional test of a full bracing bent were carried out to better understand the behaviour of this structural element, to calibrate the numerical models and to establish failure criteria to be used in the evaluation of the dynamic analysis data. Incremental dynamic analyses (IDA) of the buildings were completed with the goal of identifying the probability of failure based on brace connection failure modes for each of the buildings following a methodology that was modelled after that found in FEMA P695 (2009).

2 SINGLE-STOREY STEEL BUILDING DESIGN IN THE 1960s

2.1 1965 National Building Code of Canada (NBCC)

The National Building Code of Canada has evolved over the last 70 years as new research has emerged improving our understanding of structural behaviour and as structural design philosophy has changed from an allowable stress approach to limit states design. Load combinations for use with allowable stress design in the 1965 NBCC were as follows: 1.0D + 1.0S, 1.0D + 1.0W, 1.0D + 1.0E, 0.75(D + S + W) and 0.75(D + S + E), where D is dead load, S is snow load, W is wind load and E is earthquake load. Note that the live load and snow load were interchangeable (not cumulative). In contrast, the 2010 NBCC incorporates ultimate, fatigue and service limit states through the use of combined load effects with the companion action format. Longer return periods are applied in the determination of loads and snow (+ rain) loads have been separated from use and occupancy (live) loads, among other changes.

This evolution is especially evident in the area of seismic design and in the evaluation of seismic hazard. As such, the evaluation of seismic design force levels (represented by base shear) has advanced with each publication of the NBCC (Mitchell et al. 2010). In the 1965 NBCC the design lateral loading due to earthquake, V, was calculated as:

$$V = KW \quad \text{with } K = R\,C\,I\,F\,S \tag{1}$$

where W is the seismic weight (dead load), R is a geographical earthquake factor, C is the construction-type factor, I is the importance factor, F reflects the foundation/soil conditions and S is the structural flexibility factor (a function of the number of storeys). The design lateral load was linearly distributed to respective floor levels based on building height and weight. One of the major differences between the 1965 NBCC and the most recent NBCC (NRCC 2010) is the geographical earthquake factor, R. While today, the geographical location of the building is taken into account by the use of unique spectral acceleration ordinates, in the 1965 NBCC the procedure to determine R relied on a seismic zoning map that had been introduced in the 1953 NBCC (NRCC 1953). The country was divided into four zones (0, 1, 2 & 3), each corresponding to a value for R, which equalled the zone number except for Zone 3, in which case $R = 4$. These values were chosen based

on a qualitative assessment of historical earthquake activity. Furthermore, a notable difference between the 1965 and 2010 NBCC is the discrepancy between the seismic hazard in the eastern and western regions of the country. While today it is well understood that earthquakes in eastern and western Canada are vastly different in terms of expected accelerations, frequencies, magnitudes and return periods, the 1965 NBCC failed to differentiate between the hazard in the east and west. As such, lateral force resisting systems designed for seismic loading in the lower-magnitude, higher frequency Montreal region were often identical to those designed in the higher-magnitude, lower frequency Abbotsford region. Today, the difference in predicted ground motions in eastern and western Canada is substantial; for example the spectral acceleration for short period structures (0.2 to 0.5 sec) as per the 2010 NBCC spectral acceleration ordinates for Abbotsford is 0.35 g (55%) higher than in Montreal. Moreover, for these two cities the increase in spectral acceleration for longer period structures is 0.18 g (128%) and 0.123 g (262%), respectively for the spectral ordinates at 1.0 and 2.0 sec. Consequently, seismic forces as calculated today in western Canada are almost always significantly higher than in eastern Canada for a given structural framing system.

Differences between the calculated seismic base shear from the 1965 NBCC and the 2010 NBCC are substantial. One of the first discrepancies between the two designs is the calculation of the seismic weight, W. Even with identical assumed dead load, D, the seismic weight calculated using the modern code is higher due to the inclusion of snow loads, which has a direct impact on the magnitude of the base shear. All other factors considered, the increase in base shear V using today's design approach for single-storey steel concentrically braced frame structures is up to 1.7 times higher for moderate ductility (MD) systems, 2.5 times higher for limited ductility (LD) systems, and most importantly, 3.3 times higher for conventional construction (CC) (Caruso-Juliano 2012). Note, these values were determined based on a comparison of the 1965 and 2010 seismic loads for the 16 CBF buildings described in Section 2.3 of this paper. Conventional construction design philosophy in the 2010 NBCC and CSA S16-2009 does not require capacity design calculations; the only seismic requirement is that connections and diaphragms located along the lateral load carrying path be detailed in a ductile manner. If this is not possible then these elements are to be designed to resist gravity loads in combination with seismic loads multiplied by the ductility related seismic force modification factor R_d. The equivalent static design approach may be used for CC structures, which is similar in some respects to the design method which an engineer would

have implemented in the 1960s, however over the past five decades there certainly have been improvements in the design approach including the introduction of ductile connection detailing, more accurate seismic hazard assessment and modelling techniques, and the use of limit states design, among other aspects.

Lateral loading on a building can also be attributed to the actions of wind. The basic regional wind speed values were obtained from Supplement No. 1 of the 1965 NBCC. These speeds were converted to pressures using an empirical equation in which the constant was dependent on air temperature and atmospheric pressure:

$$W = 0.0027\, v^2 \tag{2}$$

where W is the expected wind pressure in pounds per square foot and v is the wind speed (mph). In combination with the tributary area, A, for the building in question, this pressure was converted to a lateral force, F, using Eq. 3.

$$F = W\, C_h\, C_p\, A \tag{3}$$

where for single-storey buildings with heights ranging from 4 m to 10 m the coefficient with respect to variation in height, C_h, is 1.00 and the pressure factor, C_p, is 0.85. For a single-storey building the horizontal shear at the roof level is calculated using an area, A, equal to one half the building height multiplied by the width or length of the building, depending on the wind direction under consideration.

Climatic data to be used in accordance with the 1965 NBCC was also included in Supplement No. 1. The total roof snow load to be considered for a given region was calculated as:

$$S = C_s\, GSL \tag{4}$$

where GSL is the ground snow load, and C_s is the basic snow load coefficient accounting for exposure to wind, effect of roof slopes exceeding 30^o and the accumulation of snow.

2.2 1965 Canadian Standards Association (CSA) S16 Steel Structures for Buildings

The Canadian Standards Association (CSA) S16-1965 Standard (1965) is different from modern steel design standards in many ways. Firstly, the allowable stress design approach was followed, as opposed to the limit states design philosophy currently employed in CSA S16-2009 (2009). For the purposes of designing the bracing elements and the surrounding gravity system the relevant sections of the S16-1965 are; Cl. 15 - Slenderness Ratio, Cl. 16 - Allowable Stresses and Cl. 17 - Combined Stresses.

Clause 15 specifies a maximum slenderness limit of 300 for bracing members, which was specified more for serviceability considerations; it was commonly not considered in design. Clause 16 describes the theory behind allowable stress design; in accordance with the 1965 NBCC several load combinations were required to be considered. Clause 16 is further divided into the allowable stress design for axial tension, axial compression, shear and bending (CSA, 1965).

The design of tension members, i.e. the single angle braces in the buildings of study, in CSA S16-1965 is governed by the maximum stress, F_t, on the net area reaching either $0.6F_y$ or $0.5F_u$, with a 1/3 factor stress increase permitted due to the short term nature of the lateral loads. This stress requirement can be rewritten in terms of a tension resistance as follows:

$$T_r = \min\begin{Bmatrix}(0.60+1/3\times 0.60)F_y A_n\\(0.50+1/3\times 0.50)F_u A_n\end{Bmatrix} = \min\begin{Bmatrix}0.80F_y A_n\\0.67F_u A_n\end{Bmatrix} \quad (5)$$

where A_n is the net cross sectional area, T_r is the tensile resistance, F_y is the yield stress and F_u is the ultimate tensile stress. The effect of shear lag on a tension member, which in the CSA S16-2009 often results in a reduction in resistance, was not considered in the 1965 Standard. Given the use of single angles as brace members modern standards would require a potential decrease in net-section resistance of 20% to 40% due to shear lag assuming that the bolted connection was limited to a single leg of the member; as such, larger angle braces would be required today.

CSA S16-1965 also provides values for the allowable stresses for members in axial compression. Although the principle of separating the limiting axial compression stress into separate buckling behaviour categories is similar to modern design guidelines, the empirical equations differ from

the current column curve, and consequently the gravity columns designed with the 1965 S16 would be different from those designed using the 2009 S16. The allowable compression stress F_a values determined as a function of the member slenderness are as follows:

$$\frac{kL}{r} \le C_o \ then \ F_a = 0.60F_y \tag{6}$$

$$C_o < \frac{kL}{r} \le C_p \ then \ F_a = 0.60F_y - m\left(\frac{kL}{r} - C_o\right) \tag{7}$$

$$\frac{kL}{r} > C_p \ then \ F_a = \frac{149000}{\left(\frac{kL}{r}\right)^2} \tag{8}$$

where r is the radius of gyration of the section, k is the effective length factor, L is the unbraced length, and:

$$C_o = 20 \text{ when } F_y \le 50ksi, \ and \ C_o = \left(30 - \frac{F_y}{5}\right) \text{ when } F_y > 50ksi \tag{9}$$

$$C_p = \frac{535}{\sqrt{F_y - 13}} \tag{10}$$

$$m = \frac{6.77 + 0.079F_y}{C_p - C_o} \tag{11}$$

In terms of the flexural limiting stresses for beam members, both for tension F_{bt} and compression F_{bc}, the CSA S16-1965 Standard lists values for compact I-type sections, as follows:

$$F_{bt} = 0.66F_y \tag{12}$$

$$F_{bc} = greater \text{ of :}$$
$$\frac{12000A_{fc}}{Ld} \le 0.66F_y, \ and \tag{13}$$
$$0.66F_y\left(1.18 - 0.00091\sqrt{F_y}\frac{L}{r}\right) \le 0.66F_y \ or \ \frac{149000}{(L/r)^2}$$

and for non-compact I-type sections, as follows:

$$F_{bt} = 0.60F_y \tag{14}$$

F_{bc} = *greater* of :

$$\frac{12000A_{fc}}{Ld} \le 0.60F_y, \text{ and} \qquad (15)$$

$$0.60F_y\left(1.30-0.0010\sqrt{F_y}\,\frac{L}{r}\right) \le 0.60F_y \text{ or } \frac{149000}{(L/r)^2}$$

Where, A_{fc} is the compression flange area, L is the unsupported length of the compression flange, d is the section depth and r is the radius of gyration of a tee-section comprising the compression flange and 1/6 of the web.

The allowable stresses for load cases involving axial compression and bending of the perimeter columns are provided in Cl. 17 of the 1965 CSA S16, and are written as follows:

$$\frac{f_a}{0.60F_y}+\frac{f_b}{F_b} \le 1.0 \text{ at locations braced in the plane of bending} \qquad (16)$$

$$\frac{f_a}{F_a}+\frac{f'_b}{F_b} \le 1.0 \text{ on the unbraced length when } \frac{f_a}{F_a} \le 0.15 \qquad (17)$$

$$\frac{f_a}{F_a}+\frac{f'_b}{F_{b\left(1-\frac{f_a}{F'_e}\right)}} \le 1.0 \text{ on the unbraced length when } \frac{f_a}{F_a} > 0.15 \qquad (18)$$

Where, f_a is the computed axial unit stress, f_b is the computed bending unit stress, f'_b is the equivalent bending unit stress assumed to act on the unsupported length, F_a is the axial unit stress permitted if axial force alone existed, F_b is the compressive unit stress permitted if bending moment alone existed, and $F'_e = 149000 / (kL/r)^2$ for which kL/r is the equivalent slenderness ratio in the plane of bending.

2.3 Design of single-storey CBF buildings using the 1965 NBCC and CSA S16-1965

Since the objective of the study was to obtain a general overview of the seismic performance of single-storey CBF buildings three representative cities in which this type of building would often be located, with different seismic hazard, were selected. Abbotsford was chosen as the representative west-coast city for this study because of the high seismic risk and the large snow load prescribed in the 2010 NBCC, with the goal of maximizing the potential earthquake force soliciting the archetypical buildings. Similarly, Montreal was chosen as the representative city in

the east of Canada because of the moderate seismic risk combined with the large snow loads. Halifax was chosen because it is a major east-coast city with significant building stock and is representative of a lower seismic hazard region of the country.

The study was limited to single-storey structures rectangular in plan, and with constant roof height. Dimensions were selected based on a study performed by Tremblay & Rogers (2005), in which the buildings were categorized based on total area, aspect ratio (i.e. building plan length vs. width), length, width and height (Table 1). Building areas varied between 600, 1800, 3000 and 4200 m^2. Similarly, aspect ratios of the building footprint varied between 1.0, 1.5, 2.0 and 2.5. Building heights were increased from 4.0 to 10.0 m in 1.0 m increments. It was assumed that bay sizes were consistent throughout the perimeter of the building in order to reduce the total number of building combinations considered. With the goal of eliminating redundancy of the archetypical buildings, the elastic building period was chosen as the primary attribute used in grouping similar buildings. Preliminary 1965 designs were carried out for a larger set of buildings. The period of vibration for each structure, without an upper limit, was calculated using a method proposed by Medhekar in which the flexibilities of the roof diaphragm along with the vertical braces were taken into account (Medhekar 1997; Tremblay & Bérair 1999). From this, the 16 representative buildings were selected for study (Caruso-Juliano 2012). The set of buildings was then designed separately for the three cities of interest using the 1965 NBCC and CSA S16-1965 with member sizes and cross-sectional properties obtained from the Canadian Institute of Steel Construction (CISC) Steel Construction Series Book Two (1965) (Caruso-Juliano 2012, Gallagher 2012).

A uniformly distributed dead load of 1.12 kPa, composed of 4 ply asphalt and gravel on steel deck with rigid foam along with a suspended ceiling, ductwork and fire protection, as well as the steel structure including open web steel joists and Gerber beams, was considered to act on the roof of all buildings. Additionally, the exterior walls were assumed to have a dead load of 1.5 kPa; the component of this dead load acting on the top half of the walls situated perpendicular to the direction of loading was added to the gravity load on the roof for the determination of W for seismic calculations. This approach was followed because it was assumed that the walls located parallel to the direction of loading would be able to transfer the dynamic loading resulting from their self weight through to the foundation, whereas the walls positioned perpendicular to the direction of loading would have to rely on the roof diaphragm, and subsequently the vertical bracing bents to

transfer their inertial effect to the foundation. Earthquake loads were obtained using Eq. 1; R was based on the location, Halifax (=2), Montreal (=4) and Abbotsford (=4), C = 1.25 for CBFs, I = 1.0 for buildings of regular importance buildings, F =1.0 for regular soil conditions (not highly compressible) and S was set equal to 0.025 for single-storey buildings. The lateral wind loads were calculated with Eq. 2 where v = 90 mph (Halifax), 75 mph (Montreal) and 90 mph (Abbotsford), which equated to pressures of 1.05 kPa, 0.73 kPa and 1.05 kPa, respectively, for the three cities prior to application of the C_h and C_p factors. In the 1965 NBCC live loads and snow loads were grouped together under one category. As such, the gravity load distribution for a roof structure was consistently governed by snow and dead loads. Consequently, live loads were not relied on for design. The roof snow loads, determined with a C_s factor of 0.80, were 1.73 kPa (Halifax), 2.07 kPa (Montreal) and 1.92 kPa (Abbotsford).

The lateral force resisting system consisted of CBFs with single angle tension-only braces along exterior walls. Tension-only acting X-bracing was symmetrically placed along each of the four perimeter walls, with a single bracing bent required per wall. All braces were single angles connected together at mid-length and bolted (ASTM A307 (2012) equivalent snug-tight bolts) to gusset plates at each end. No ductility verifications were performed in the member and connection selection and design, which is consistent with design in the 1960s. The roof deck panels were selected based on design for gravity loads alone. In the 1960s it was not standard practice to determine the shear resistance of the roof diaphragm. A typical roof deck was chosen according to that commonly found in building design in the 1960s: 22 gauge (0.76 mm thick) – 38 mm deep × 914 mm wide corrugated deck with six 152 mm wide flutes, assumed to have F_y = 230 MPA, F_u = 310 MPa and E = 200000 MPa. The fastener pattern was a button punch side-lap at 600 mm o/c and 19 mm diameter arc-spot welds on supports at 300 mm o/c (pattern 914/4 = every second flute). The various building configurations had a joist spacing that varied from 1.667 m to 2.025 m depending on the bay size.

The gravity load carrying system considered in the 1965 design comprised open web steel joists, supported on cantilevered Gerber beams for the interior spans, with simply supported perimeter beams and I-shape columns. All beams were designed considering gravity loads alone, while the exterior building columns were designed taking into consideration the applied gravity and wind loading (both normal to and in the plane of the braced bent), as well as gravity and seismic loading

(in the plane of the braced bent). Interior building columns were designed based on gravity loading alone. Standard size I shaped beams and columns of the 1960s included both wide flange (WF) shapes, now known as W-sections, and standard American (B) shapes, now known as S-sections. In-plane torsional effects were not included in the design and analyses, nor was consideration given to column uplift and foundation design.

Specific member sizing for all 48 buildings was carried out based on the allowable stress limitations described in Section 2.2 for the 1965 CSA S16 Standard and by taking a least weight design approach through the use of the selection tables found in the First Edition of the CISC Handbook of Steel Construction (1967). Member sizes for the brace, beam and column members in the bracing bent of each building are listed in Table 2; additional information can be found in the reports of Caruso-Juliano (2012) and Gallagher (2012). The structural steel was assumed to be of CSA Grade G40.12 (1964) with material properties for design as follows: F_y = 300 MPa, F_u = 450 MPa and E = 200000 MPa.

3 EVALUATION OF TYPICAL ANGLE BRACE CONNECTIONS

Tests were conducted on angle braces (with bolted connections), that were extracted from the PMQ Sector 4 Rio Tinto facility constructed in 1967 in Sorel-Tracy, Québec, using a reversed cyclic testing protocol from FEMA 461: Interim Protocol I – Quasi-Static Cyclic testing (FEMA 2007) (Caruso-Juliano 2012) prior to the dynamic modelling of the representative buildings. The intent was to measure the response of these representative 1960s braces to simulated seismic loading such that the numerical models could be calibrated accordingly and to identify the potential failure modes and ductility capacity of these members and their connections. It was observed that net section fracture in the braces of varying ductility appeared as the dominant failure mode. As well, there was no gross yielding over the entire brace length, only concentrated plasticity in the net-section at the bolted connection (Figure 3). The most brittle net-section fracture occurred at 0.39% elongation of the length of the test brace, but elongations were observed up to 1.85% for the existing braces when net section fracture occurred without yielding of the gross section away from the connection. These test results were used in the calibration of the hysteretic brace elements used in the OpenSees models. Other failure types that could occur in a single-angle CBF under tension

loading include; bolt shear, block shear, bearing and gross yielding of the angle braces. These failure types have been observed in tests of angles carried out by Hartley (2010) and Castonguay & Tremblay (2010), and are summarized in the paper by Hartley et al. (2012). The Castonguay & Tremblay study involved the monotonic tension testing of various double-angle connection configurations with the goal of producing the desired failure type; gross yielding along the entire member length, block shear rupture at the connection, bolt shear fracture and bearing failure in the connection. In addition to the net-section fracture tests by Caruso-Juliano (2012) the results of these additional tests were relied on to define the criteria by which failure was deemed to have taken place for the evaluation of the dynamic analysis results.

4 SINGLE-STOREY BUILDING DYNAMIC ANALYSES

Numerical dynamic models of the 48 different single-storey buildings (16 for each of the three cities) were created using OpenSees. The drift demand was then studied by subjecting each building to a series of 20 earthquake records by use of non-linear time history dynamic analyses using an incremental dynamic analysis approach. The lateral force resisting system consisted of CBFs along exterior walls with single angle bracing and included the steel roof deck, which was assumed to act as a flexible diaphragm to transfer lateral loads to the CBFs, even though it would not have initially been designed for this purpose in the 1960s. The study was limited to structures on soils of class C and the seismic mass was determined as defined in the current NBCC (NRCC 2010). Torsional effects were not accounted for since the buildings were rectangular or square and symmetrical in plan with uniform mass, lateral stiffness and lateral strength. The effect of non-structural components, including cladding and interior partitions, on the dynamic response was not included. Lastly, the rigidity of beam-to-column connections and the influence of column uplift at foundations were not accounted for in the models.

4.1 Numerical building model

The numerical model of the representative buildings (Figure 4a) included the lateral force resisting structure in the braced bent and the flexible roof deck diaphragm. Due to symmetry, only half of each building was modelled. Gravity members that were assumed not to contribute to the lateral

behaviour of the structure were excluded. Similar in modelling configuration to that used by Medhekar & Kennedy (1999) elastic co-rotational P-Δ columns of relatively rigid axial stiffness, pinned at the base, were assigned a tributary portion of the seismic weight, $P_{P\Delta}$, to simulate P-Δ forces over the span of the diaphragm. The dead load of the top half of the wall was assumed to contribute to the seismic weight, along with the roof mass and snow, but only for walls placed perpendicular to the direction of the load. An additional tributary gravity load P_{trib}, which was not part of the seismic weight, was placed above the two columns in the braced bent.

The braced bent was composed of elements to represent the braces, brace connections, gusset plates, beam, columns and beam-to-column connections. Based on Agüero (2006) each half-length of single-angle brace incorporated eight non-linear beam-column fibre elements (A & E) (Figure 4b) such that bi-axial bending as well as axial load and buckling effects were included. These elements contained 10 fibres across the length and 4 across the thickness of each angle leg (Figure 5b). A material property of Steel02 was assigned which accounted for isotropic strain hardening (Figure 5a). Buckling behaviour was initiated by off-setting the centre node of each brace in the z-direction by $L/500$, where L is the total brace length. The brace intersection was represented by two zero-length elements, C, with effectively rigid material properties to simulate a stiff connection. The two nodes were linked with an equal degree of freedom master-slave arrangement.

Brace element A was connected to the surrounding gravity frame by means of a zero-length spring (element B) to simulate the axial and rotational stiffness of the gusset plate and an axially rigid elastic beam-column element link to represent the length of the gusset plate. Elastic material properties were assigned to the zero-length elements to reproduce the axial stiffness of the gusset plate, while the out-of-plane rotational stiffness was represented using the Steel02 material. The zero-length gusset plate element was used to simulate the flexible gusset plate region at the end of the brace (of length $2t_g$, where t_g is the thickness of the gusset plate) while the axially-rigid link represented the rigid region of the gusset plate which exists beyond the $2t_g$ region. Note, this flexible region in the gusset plate was not always detailed for braced frame buildings in the 1960s because the importance of ductile detailing was not necessarily recognized at the time. However, since the braces tested by Caruso-Juliano (2012) were constructed with a flexible gusset plate it was decided to replicate the detail in the building model.

The rigid-link was connected to the beam and columns in the bracing bent (elements D). These frame members were modelled using elastic beam-column elements having the cross-sectional properties of the I-section members chosen in the building design. The beam-to-column connections were modelled by means of a zero-length rotational spring, assigned a very low rotational stiffness relative to the rest of the model with the goal of simulating a pinned connection. A true pinned joint was not used due to convergence issues associated with having an infinitely flexible connection in the model. It was assumed for these models that the force levels in the beam and column members (elements D) would remain elastic. This was confirmed under the design-level earthquake events by use of the recorded forces and the elastic beam-column interaction equations found in CSA S16 (2009).

The roof diaphragm was modelled as an elastic beam system with realistic in-plane flexural and shear stiffness (Figure 4a). Horizontal beam-column elements were interconnected with translational horizontal springs at the column positions, which characterize the roof diaphragm shear stiffness. These zero-length elements were assigned a stiffness in the direction of lateral loading based on the specified diaphragm shear stiffness, G', as calculated using the Steel Deck Institute (SDI) method (Luttrell 2004). The flexural stiffness of the diaphragm was represented through the use of elastic beam-column elements connecting each of the diaphragm translational springs. These elements were assigned a value of I about the local z-axis equal to the calculated diaphragm moment of inertia based on the depth of the roof and area of the chord members (beams) in the building. To ensure continuity of the flexural effects in the diaphragm the zero-length shear elements were assigned high stiffness in the axial direction of the beam elements as well as high rotational stiffness. The P-Δ co-rotational columns were pin connected to the elastic beam diaphragm elements.

The analysis time step was taken as 1/30 of the ground motion time step. The tolerance for the iterations of the analysis was set to 0.0000001, and the maximum number of iterations at 500. The solution algorithm used was the Modified Newton, and the integrator was Newmark-Beta with alpha and beta parameters set to 0.5 and 0.25 respectively. The damping in the system was modelled using an initial stiffness Rayleigh approach with a damping coefficient, ξ, of 2% in the

first and third modes. These parameters were selected by means of a sensitivity analysis to ensure the accuracy of the converged numerical solution.

4.1.1 Brace element calibration

The brace calibration was performed by creating a separate numerical model consisting of the gusset plates and brace elements to replicate the setup used in the physical tests (Caruso-Juliano 2012). The axial deformation of the gusset plate had to be accounted for; an elastic material in the axial direction was added to the gusset plates to match the global elastic stiffness of the brace specimens and to provide accurate deformation data. A value of E/1.5 was selected as the material stiffness of the gusset plate in the axial direction, which produced closely matching elastic slopes between the physical tests and the numerical OpenSees model. The value was chosen to specifically match the axial rigidity of the gusset plates used in the laboratory tests.

Additionally, the physical testing of the specimens demonstrated the inability of the 1960 braces to undergo global-yielding of the gross cross-section along the length of the brace member. Rather, each specimen yielded locally at the net-section and soon there-after fractured. The model replicated this yielding across the net-section prior to yielding along the length of the brace. Reducing the physical area of the element at the net section caused problems related to the lateral stiffness of the structure, as well as the compression stiffness of the element. Consequently, an alternative was used, in which the end element, A, of each half brace was given a lower yield stress value, calculated as:

$$F_{effective} = 0.6\ F_u\ 0.85 \tag{19}$$

where F_u is the ultimate stress of the angle brace taken from the coupon tests, 0.6 is the shear lag factor prescribed in CSA S16 (2009) and 0.85 was chosen as the representative ratio of the net to gross cross-sectional area, based on the bolt configurations of the test specimens. The cross-sectional area of element A was not reduced even though bolt holes exist in the angle brace. By having the end element, A, yield at lower force levels than the rest of the brace elements, B, it was ensured that the total axial deformation was representative of only the net-section yielding, as opposed to the much larger deformations which would be present had the gross cross-section

yielded in tension along the length of the brace. The model was able to accurately replicate the resistance vs. deformation hystereses behaviour of the test specimens (Figure 5a) and the energy dissipation (Caruso-Juliano 2012). It is worth noting that the physical test specimens exhibited bolt-slip upon load reversal (snug-tight bolts were installed), while the model did not capture this behaviour. As a result, the load in the model increased immediately upon load reversal, while in reality the specimen first had to displace to overcome the bolt-slip. The model typically exhibited higher dissipated energies in the early elastic range. However, upon overcoming the bolt-slip and entering the inelastic range, the model and the physical test resulted in matching dissipated energies.

Furthermore, Morrison (2013) carried out a reversed cyclic test of a representative braced bent (Figure 6b) in order to verify the calibration of the numerical OpenSees models, however in this case the objective was to obtain a lateral force vs. drift hysteresis of single angles (L127x76x9.5) in an X configuration up to the 4% drift level. Since this level of drift was not attainable given the common detailing used in the 1960s it was decided to use recently fabricated angles for which the yield stress and the F_u/F_y ratio were such that yielding in tension over the gross cross-section along the brace length would occur prior to connection failure. A numerical model of the braced bent was developed (Figure 6a), as per that described in Figure 4b. A comparison of the hysteretic force vs. displacement response along with the dissipated energy vs. cumulative displacement is provided in Figures 6c and 6d, respectively. These figures demonstrate the ability of the fibre brace model to capture the response of the braced bent even at large drifts with extensive buckling of the single angle braces.

4.1.2 Failure criteria of brace elements in building models

It was necessary to establish realistic failure levels based on non-simulated considerations since strength degradation was not explicitly accounted for in the building models. Collapse under each ground motion was judged to occur either directly from dynamic analysis results as evidenced by excessive lateral displacements or assessed indirectly through non-simulated component limit state criteria. Thus, the incremental dynamic analyses performed in this study were representative of the insipient collapse, and not the actual collapse of the structures.

Seven major design failure criteria were identified, each one represented a different mode of brace member or brace connection failure, including; net section fracture, bearing failure, block shear rupture, bolt shear fracture and brace member yielding in the gross section. Note, the brace yielding mode of failure would likely not be attainable for the typical single-storey structures constructed in the 1960s because capacity based design and ductile detailing requirements were not part of the seismic design process. Nonetheless, it was included as a failure criterion to demonstrate the building response if structural rehabilitation had been completed of the existing brace connections and bracing bay members, along with other affected structural components. Compression related failure of the single angle braces was not of concern given their large overall slenderness and because there are no reported issues with low cycle fatigue induced fracture initiated by local buckling as seen for stockier HSS and I-shape braces. Based on the ultimate deformation values of the angle brace tests by Caruso-Juliano net-section fracture was divided into three categories (Table 3). Ultimate deformation values for the other failure mechanisms were obtained from Castonguay & Tremblay (2010). The test results for each of these failure mechanisms were averaged to obtain a singular value for the ultimate elongation, δ_u, and the corresponding ultimate force, P_u. However, the lengths of the test specimen braces were not equivalent to those for the braces in the 16 archetypical buildings. A full-length brace would have had a longer section with which to deform elastically; for this reason the ultimate deformation values of the Caruso-Juliano and Castonguay & Tremblay tests were adjusted to reflect the longer brace sections in the buildings. This was done by subtracting the elastic deformation along the length of the test specimens to obtain the connection deformation (combined for both brace ends), δ_{Conn}, using Eq. 20:

$$\delta_{Conn} = \delta_{Measured} - \delta_e = \delta_u - \frac{P_u L}{EA} \tag{20}$$

Where δ_u is the elongation of the entire specimen during testing at the point when the ultimate axial force in the specimen, P_u, is reached, L is the original length of the test specimen, E is Young's modulus and A is the gross area of the brace section. A new elastic deformation was then re-calculated by adding the elongation of a full length brace to the connection elongation at each end. In this case L was the full-brace length and A was the gross area of the single-angle section being used for the specific building under consideration. In making this adjustment, realistic values

for the ultimate deformation, δ_{ult}, which include both brace and connection elongations were obtained for all failure types. Consequently, the normalized ultimate axial brace deformation values, δ_{ult}/L, were determined for each of the 16 building sizes (Table 1) given the associated brace length. For illustrative purposes Table 3 contains a listing of the average brace elongation, of the 16 buildings, as a percentage for each failure type. Note, these average values were not used in the evaluation of the building response; rather, the specific brace elongation for each building and failure type was translated into an equivalent lateral drift using the geometry of the braced bent and then utilized in determining whether the building would have withstood the applied ground motion. It was determined that the gross yielding of the brace along its length, produced an equivalent building drift larger than the 2.5% limit imposed by the 2010 NBCC; as a result, the 2.5% storey drift was used as a final criterion for failure. It is important to note, however, that none of the tested braces exhibited the ability to yield as would be required to reach this 2.5% building drift; instead failures at the net section, of the bolts, etc., would occur at substantially smaller drifts. The purpose of including this final criterion was to demonstrate the building performance if the other failure modes could be avoided by means of reinforcement. Without some sort of structural remediation it would be unlikely that this 2.5% drift would be attainable by the single-storey buildings studied for this research project.

4.2 Earthquake ground motion records

Earthquake ground motions were selected as part of a joint-effort of the Canadian Seismic Research Network in order to ensure consistency of dynamic analysis results for the various steel building research projects. A separate suite of 10 historical ground motions and 10 simulated earthquake records were chosen for both western and eastern Canada based on guidelines for the selection and scaling of time histories as presented by Atkinson (2009). The simulated records were selected using records from Atkinson's database (2009) near the large end of the distance range for each magnitude for eastern Canadian sites of low seismicity; magnitude 6 and 7. The historical records were selected from a database of earthquake records by McGuire (2004). The earthquake records were scaled such that their response spectra were matched to the uniform hazard spectra presented in the NBCC 2010 for Halifax, Montreal and Abbotsford for Class C soil

conditions, and for the 2% in 50 year return period prescribed in the 2010 NBCC (Tables 4-6, Figure 7). Note, the ground motions were applied in the short direction of the building models.

4.3 Response of representative buildings to ground motions

4.3.1 Effect of seismic loading on the roof diaphragm

A significant portion of the mass in a single-storey building is located in the roof structure and in the upper portion of the building's walls. Hence, it is necessary to transfer the seismic forces that develop due to this mass through the roof structure to the braced bents. The archetypical buildings were designed without consideration of the need to transfer these seismic forces. Roof deck panels were connected as per the common configuration in the 1960s, i.e. 0.76 mm thick × 38 mm deep corrugated panels with 600 mm side-lap fastener spacing and 19 mm arc-spot welds in a 914/4 pattern. A horizontal truss system could have been placed in the roof structure to act as a load carrying device; however, buildings of this era were not necessarily designed in this fashion. Prior to completing the incremental dynamic analyses an evaluation was carried out as to the effectiveness of the standard 1960s roof as a diaphragm, which was postulated to remain in the elastic range of behaviour while undergoing the applied loading based on the 2010 design level UHS scaled ground motions. A representative example for a single ground motion applied to an Abbotsford building is shown in Figure 8, where the calculated shear forces exceed the SDI shear resistance (Luttrell 2004). This finding demonstrated the need for the retrofit of the roof diaphragm of these buildings such that the lateral forces obtained from ground motions scaled to current design 2010 NBCC levels could be transferred to the braced bents. Since the main purpose of the research was to evaluate the performance of the buildings as a function of their lateral braces and brace connections the connection pattern in the roof structure was modified, as would be recommended by an engineer in a building seismic upgrade. The deck-to-frame connection pattern was changed, for example, from a 914/4 (every second flute is connected) to a 914/7 pattern (every flute is connected) and additional side-lap fasteners were installed such that the spacing was reduced to 150 mm from 600 mm. The same roof deck connection pattern was used throughout the roof structure. With these adjustments, the diaphragm's factored shear resistance for this particular representative building was increased to 16.2 kN/m from 8.1 kN/m, while the shear stiffness was only marginally increased to 9.5 kN/mm from 9.2 kN/mm. Because the shear stiffness

remained essentially unchanged, the period of vibration of the structure and consequently its dynamic response were unaffected. This process was undertaken for all buildings in the study such that an elastic diaphragm response was obtained and the behaviour of the building could be evaluated as a function of the brace elements.

4.3.2 Probability of failure

Incremental dynamic analyses for all buildings and cities were completed. The failure criteria associated with brace elongation, as demonstrated by the average values listed in Table 3, were used in the performance evaluation process. Note, the brace failure criteria specific to each building size were converted to a lateral drift in order to compare with the results of the dynamic analyses. The ground motion records were systematically scaled in intensity in a step-wise fashion (+0.2 for each step) until the median collapse was established; scaling factors of 0.2 to 6 for Montreal and Halifax and 0.2 to 3 for Abbotsford were used. FEMA P695 (2009) defines the median collapse intensity, S_{CT}, as the ground motion intensity at which half of the earthquake records cause failure to occur. The ratio between S_{CT} and the maximum considered earthquake (MCE) ground motion intensity, S_{MT}, is defined as the collapse margin ratio, CMR. The CMR is the primary parameter used in assessing the collapse safety of a structure; a value was calculated for each archetypical building and failure type as the being equal to S_{CT} because $S_{MT} = 1.0$ due to the pre-scaling of all ground motions to the design UHS of the 2010 NBCC of the respective city prior to running the IDAs. A separate fragility curve for each combination of building and failure type, examples of which are found in Figure 9, was then constructed using a lognormal fit of the IDA results, corresponding to the collapse probability versus the scaling factor. These fragility curves, which represent the probability of failure for each of the buildings, and the CMR were then adjusted to account for the various uncertainties present in the analysis. Two adjustment factors were used: the spectral shape factor, SSF, and the total collapse uncertainty, β_{tot}. The SSF is a function of the ductility capacity, μ_T, and the fundamental period of the structure, T, and was obtained from Table 7-1a of FEMA P695 (2009) for archetypical buildings designed for US seismic design categories B, C or D_{min}, which were deemed to be a reasonable match to the seismic hazard for the three Canadian cities of interest. The ductility μ_T, was calculated as the ultimate lateral deflection, Δ_u, unique to a particular failure criteria, divided by the yield deflection, Δ_y, of the building. Thus,

each of the seven selected failure criteria for each of the 48 buildings had a unique μ_T, and consequently, a unique value for SSF. The value of $\beta_{TOT} = 0.80$ (Eq. 21), which is the lognormal standard deviation of the uncertainty-adjusted fragility curves for all buildings, was identified as follows: $\beta_{RTR} = 0.40$, record-to-record uncertainty; $\beta_{DR} = 0.3$, design requirement uncertainty was defined as 'good' according to FEMA P695 due to the desire to simulate the performance of existing buildings; $\beta_{TD} = 0.45$, test data uncertainty was evaluated as 'fair' because only a limited number of 1960s braces were tested, and; $\beta_{MDL} = 0.45$, the modelling uncertainty was judged to be 'fair' because the model does not explicitly account for strength and stiffness degradation mechanisms, and consequently does not have collapse capabilities.

$$\beta_{tot} = \sqrt{\beta_{RTR}^2 + \beta_{DR}^2 + \beta_{TD}^2 + \beta_{MDL}^2} \tag{21}$$

By applying Eq. 22 the adjusted collapse margin ratio (AMCR), which becomes the mean of the adjusted fragility curve, was obtained.

$$ACMR = CMR \times SSF \tag{22}$$

Acceptance criteria were based on the probability of collapse using the adjusted collapse margin ratio, ACMR, and comparing it to acceptable values $ACMR_{10\%} = 2.79$ and $ACMR_{20\%} = 1.96$ as provided in Table 7-3 of FEMA P695 (2009) for $\beta_{TOT} = 0.80$. The requirement is for the average $ACMR \geq ACMR_{10\%}$ and the individual values of $ACMR \geq ACMR_{20\%}$. A summary of the results showing the percentage of buildings meeting the acceptable performance level $ACMR_{20\%}$ for each individual building is provided in Table 7. Tables 8, 9 and 10 contain the calculated ACMR values specific to each building in each city, as well as the average for each failure mode. In the seismic evaluation of a single-storey building an engineer would need to identify the anticipated failure mode of the existing structure a priori based on calculations and engineering judgement. In the case of net section fracture coupon tests, providing measured ductility and F_u/F_y ratio, would likely be needed to categorize which would occur. With this information it is possible to observe the percentage of the 16 buildings that would have met the P695 acceptable performance level. For example, if it is shown that the brittle net section fracture of the braces (Category 1) is expected then none of the buildings in Abbotsford would have survived the 20 ground motions, 13% of the buildings in Montreal would have survived and 94% of the buildings in Halifax would have

survived. However, if a more ductile form of the same failure mode (Category 3) is expected then all of the 16 archetypical buildings in Montreal and Halifax would be able to meet an acceptable performance level.

It was determined that for Abbotsford the performance of the CBF buildings was unsatisfactory for the first six failure criteria, while the same buildings analysed for earthquake ground motions calibrated to the Montreal UHS performed better, yet in many cases only 38% or less of the buildings had acceptable performance. This is due to the fact that although the seismic design criteria were the same for these two cities in 1965 the uniform hazard spectrum specified in the 2010 National Building Code of Canada is more demanding for Abbotsford. While the performance of the Abbotsford structures was unacceptable for the stricter failure criteria, the buildings performed reasonably well when it was assumed that the braces had sufficient inelastic capacity to resist the 2.5% drift level prior to any strength loss. For Halifax, in general, although 100% acceptable performance was not achieved in all cases, the 16 single-storey steel structures designed according to the 1965 NBCC and CSA S16-1965 performed well for the seven failure criteria considered in this study.

The performance evaluation procedure incorporated in this study was dependent to some extent on the FEMA P695 (2009) methodology. Recognizing that this methodology results in what can best be categorized as an approximate indicator of collapse potential of a structure, and acknowledging that it has not been thoroughly verified as to its applicability to all structural framing systems it is important to view the resulting findings of this study as providing a global overview of the seismic response of existing single-storey steel CBF framed buildings without attaining the accuracy needed to carry out the evaluation of a specific structure. Further to this, since the objective was to obtain a general overview of seismic performance of a large number of buildings it was decided to simplify the numerical models by not including the rotational stiffness of beam-to-column connections, with or without gusset plates, or the potential for column uplift to occur due to light foundations and / or anchor rod elongation. As such the redundancy in term of lateral load carrying ability and energy dissipation offered by these behaviours was not accounted for.

5 CONCLUSIONS

The performance of single-storey CBF steel structures with flexible diaphragms was examined by means of non-linear time history dynamic analysis. Forty-eight buildings, 16 of each in Halifax, NS, Montreal, QC and Abbotsford, BC, were designed using the 1965 NBCC and the 1965 CSA S16 Steel Design Standard using an approach expected of an engineer in the 1960s. These buildings were subsequently modelled in OpenSees accounting for the inelastic hysteretic behaviour of the braces and brace connections as obtained from tests of braces removed from a building built in the 1960s, as well as the anticipated elastic response of the roof diaphragm. Each building was subjected to a set of 20 ground motions first scaled to the uniform hazard spectrum of the respective city for the 2010 NBCC. Incremental dynamic analysis was carried out; the results of which were used to produce fragility curves, with which the probability of failure of the non-simulated failure criteria could be identified. These failure criteria representing the insipient collapse of the structure were obtained from tests of angle braces that failed by net section fracture, bearing failure, block shear rupture, bolt shear fracture and gross cross-section yielding. The intended performance level in the design earthquakes, as well as the acceptance criteria used in the braced frame analysis was established following a methodology similar to that prescribed in FEMA P695. It was determined that the performance of the structures designed in Abbotsford was unsatisfactory for all of the brace connection failure mechanisms. In contrast, because of the lower seismic hazard in Montreal according to the 2010 NBCC the 16 archetypical buildings demonstrated better performance considering that they had been designed in the 1960s for the same seismic loading level as Abbotsford. With respect to the representative buildings located in Halifax, although acceptable performance was not achieved in all cases, the single-storey steel structures, on average, performed well, for the seven failure criteria. It was however, necessary to upgrade the roof diaphragm of the buildings in each of the cities by increasing the number of frame and side-lap connections such that it was capable of transferring the seismic induced loads from the 2010 design level scaled ground motions to the bracing bents.

The findings described herein certainly illustrate the serious deficiencies of these existing buildings with respect to the ability to resist current earthquake hazard. However, prior to condemning the design and performance of these existing buildings as a whole it is important to realize that the modelling approach used in the study was arrived at in consideration of the large

number of computer runs that were required to carry out the incremental dynamic analyses and the objective to highlight the influence of the braces and brace connections on the seismic response. The model did not capture all of the characteristics that these CBF structures possess in terms of resisting seismic loading. A more accurate picture of the performance of an individual structure requires the introduction of realistic beam-to-column connection properties, column uplift behaviour, inelastic bracing bent beam and column behaviour along with an improved ability to capture strength and stiffness degradation as inelastic damage occurs in the structure.

ACKNOWLEDGEMENTS

The financial support of the Natural Sciences and Engineering Research Council (NSERC) through the Canadian Seismic Research Network (CSRN) is gratefully acknowledged as is the computing support provided by Calcul Québec. The authors would like to thank Hatch Ltd., Proco Inc. and Rio Tinto for the donation of the brace members and fabrication of test specimens used in calibration of the building models.

REFERENCES

Agüero, A. 2006. Modeling of the seismic response of concentrically braced steel frames using the OpenSees analysis environment. International Journal of Advanced Steel Construction, 2(3), 242-274.

ASTM. 2012. A307 Standard specification for carbon steel bolts, studs, and threaded rod 60 000 PSI tensile strength. American Society for Testing and Materials (ASTM).West Conshohocken, USA.

Atkinson, G.M. 2009. Earthquake time histories compatible with the 2005 National Building Code of Canada uniform hazard spectrum. Canadian Journal of Civil Engineering 36: 991-1000.

Bruneau, M., Uang, C., Whittaker, A. 1998. Ductile design of steel structures. New York: McGraw-Hill.

CISC. 1965. Steel Construction Series : Book Two. Properties of Shapes, Plates, Bars and Tubes. Canadian Institute of Steel Construction (CISC). Toronto, Ontario.

CISC. 1967. Handbook of Steel Construction, 1st Edition. Canadian Institute of Steel Construction (CISC). Toronto, Ontario.

CSA. 1964. G40.12 General purpose steel. Canadian Standards Association (CSA). Ottawa, Canada.

CSA. 1965. S16 Steel structures for buildings. Canadian Standards Association (CSA). Ottawa, Canada.

CSA. 2009. S16 Design of steel structures. Canadian Standards Association (CSA). Mississauga, Canada.

Caruso-Juliano, A. 2012. Performance of seismically deficient existing braced steel frame structures with flexible diaphragms. M.Eng. Thesis. Dept. of Civil Eng. & Applied Mech., McGill University, Montreal, Canada.

Castonguay, P.X. Tremblay, R. 2010. Seismic performance of concentrically braced steel frames of the conventional construction category. Research Report No. ST10-02, Group for Research in Structural Engineering, Dept. of Civil, Geological and Mining Eng., Ecole Polytechnique, Montreal, Canada.

FEMA. 2009. P695: Quantification of building seismic performance factors. Federal Emergency Management Agency (FEMA). Washington, USA.

FEMA. 2007. 461: Interim testing protocols for determining the seismic performance characteristics of structural and non-structural components. Federal Emergency Management Agency (FEMA). Washington, USA.

Gallagher, A. 2012. Seismic performance of existing braced steel frame structures with flexible diaphragms in Halifax. M.Eng. Project Report G12-39. Dept. of Civil Eng. & Applied Mech., McGill University, Montreal, Canada.

Hartley, J. 2011. Performance and retrofit of seismically deficient existing braced steel frame structures: testing of brace connections from existing concentrically braced steel frames. M.Eng. Thesis. Dept. of Civil Eng. & Applied Mech., McGill University, Montreal, Canada.

Hartley, J., Rogers, C.A., Castonguay, P.X., Tremblay, R. 2012. Inelastic seismic performance of brace connections in steel tension-only concentrically braced frames. STESSA 2012 – 7th International Conference on the Behaviour of Steel Structures in Seismic Areas; Santiago, Chile, 289-295.

Luttrell, L.D. 2004. Diaphragm design manual (3rd ed.). Steel Deck Institute. Fox River Grove, USA.

Mazzoni S., McKenna F., Scott M.H., Fenves G.L. 2009. Open system for earthquake engineering simulation; User command language manual. Pacific Earthquake Engineering Research Center, University of California, Berkeley, USA.

McGuire, R.K. 2004. Seismic hazard and risk analysis. Earthquake Engineering Research Institute, Oakland, USA.

McKenna, F.T. 1997. Object-oriented finite element programming: Frameworks for analysis, algorithms and parallel computing. PhD Thesis. Dept. of Civil Engineering, University of California, Berkeley, USA.

Medhekar, M.S. 1997. Seismic evaluation of steel buildings with concentrically braced frames. Ph.D. Thesis. Dept. of Civil and Environmental Engineering, University of Alberta, Edmonton, Canada.

Medhekar, M.S., Kennedy, D.J.L. 1999. Seismic evaluation of single-storey steel buildings. Canadian Journal of Civil Engineering, 26(4), 379-394.

Morrison, T.E. 2013. Seismic mitigation technique for existing single-storey steel CBF structures. Ph.D. Thesis. Dept. of Civil Eng. & Applied Mech., McGill Univ., Montreal, Canada.

Mitchell, D., Paultre, P., Tinawi, R., Saatcioglu, M., Tremblay, R., Elwood, K., DeVall, R. 2010. Evolution of seismic design provisions in the national building code of Canada. Canadian Journal of Civil Engineering 37: 1157-1170.

NRCC. 1953. National building code of Canada. National Research Council of Canada. Ottawa, Canada.

NRCC. 1965. National building code of Canada. National Research Council of Canada. Ottawa, Canada.

NRCC. 2010. National building code of Canada. National Research Council of Canada. Ottawa, Canada.

Tremblay, R, Bérair, T. 1999. Shake table testing of low-rise steel buildings with flexible roof diaphragms.8th Canadian Conf. on Earthquake Engineering; Vancouver, Canada, 585-590.

Tremblay, R., Rogers, C.A. 2005. Impact of capacity design provisions and period limits on the seismic design of low-rise steel buildings. International Journal of Steel Structures, 5(1): 1-22.

Table 1. General parameters of archetypical buildings for Abbotsford, Montreal and Halifax

Building[1]	*Area*	*Aspect ratio*	*L×W*	*Bay size*	h_n	t_{NBCC}[2]	t_{calc}[3]
	(m^2)		(m×m)	(m)	(m)	(sec)	(sec)
1A, 1M, 1H	600	1.0	24.5×24.5	6.12	4.0	0.20	0.61
2A, 2M, 2H	600	1.5	30.0×20.0	5.00	5.0	0.25	0.69
3A, 3M, 3H	600	2.0	34.6×17.3	5.77	6.0	0.30	0.78
4A, 4M, 4H	600	2.5	38.7×15.5	7.75	7.0	0.35	1.01
5A, 5M, 5H	1800	1.0	42.4×42.4	7.07	5.0	0.25	0.81
6A, 6M, 6H	1800	1.5	52.0×34.6	8.66	6.0	0.30	0.95
7A, 7M, 7H	1800	2.0	60.0×30.0	7.50	7.0	0.35	1.08
8A, 8M, 8H	1800	2.5	67.1×26.8	6.71	8.0	0.40	1.23
9A, 9M, 9H	3000	1.0	54.8×54.8	7.83	6.0	0.30	0.95
10A, 10M, 10H	3000	1.5	67.1×44.7	7.45	7.0	0.35	1.13
11A, 11M, 11H	3000	2.0	77.5×38.7	7.75	8.0	0.40	1.30
12A, 12M, 12H	3000	2.5	86.6×34.6	8.66	9.0	0.45	1.47
13A, 13M, 13H	4200	1.0	64.8×64.8	8.10	7.0	0.35	1.08
14A, 14M, 14H	4200	1.5	79.4×52.9	8.82	8.0	0.40	1.28
15A, 15M, 15H	4200	2.0	91.7×45.8	9.16	9.0	0.45	1.48
16A, 16M, 16H	4200	2.5	102.5×41.0	10.25	10.0	0.50	1.67

[1] A = Abbotsford, BC, M = Montreal, QC, H = Halifax, NS.
[2] Period of vibration calculated using upper limit of NBCC (NRCC 2010) equation for braced frames $t_{NBCC} = 2 \times 0.025\ h_n$.
[3] Period of vibration calculated in short direction of building using Medhekar (1997) method accounting for brace and diaphragm stiffness without upper limit.

Table 2. Bracing bent design of archetypical buildings for Abbotsford, Montreal and Halifax

Building	*Abbotsford BC*			*Montreal QC*			*Halifax NS*		
	Beam	Column	Brace	Beam	Column	Brace	Beam	Column	Brace
1	8WF20	6WF15.5	L2x1-1/2x3/16	6WF25	6WF15.5	L2x1-1/2x3/16	12B14	6WF15.5	L2.5x2x1/8
2	6WF15.5	8WF17	L2-1/2x2x3/16	6WF20	6WF15.5	L2-1/2x2x3/16	12B14	6WF20	L2.5x2x1/8
3	8WF20	10WF25	L3x2x3/16	6WF25	6WF25	L3x2x3/16	12B14	8WF24	L2.5x2.5x1/8
4	10WF33	14WF38	L2-1/2x2x1/4	12WF27	10WF54	L2-1/2x2x1/4	14B22	8WF35	L2.5x2x3/16
5	10WF25	6WF25	L3-1/2x3x1/4	8WF31	6WF20	L3-1/2x3x1/4	10WF21	6WF20	L2.5x1.5x1/4
6	14WF30	14WF30	L4x3x1/4	12WF36	8WF28	L4x3x1/4	16B26	8WF31	L2.5x2.5x3/16
7	10WF33	18WF35	L5x3x1/4	10WF33	10WF54	L5x3x1/4	12B22	8WF35	L2.5x2.5x1/4
8	10WF29	14WF43	L5x3x5/16	10WF25	8WF40	L5x3x5/16	12B16.5	8WF48	L6x3.5x1/4
9	10WF33	14WF30	L3-1/2x3x7/16	10WF33	10WF29	L3-1/2x3x7/16	14B22	8WF31	L6x3.5x1/4
10	10WF33	16WF40	L3-1/2x3x1/2	10WF33	10WF54	L3-1/2x3x1/2	12B22	8WF35	L6x3.5x1/4
11	12WF31	14WF49	L5x3x7/16	12WF31	18WF45	L5x3x7/16	14B22	8WF48	L6x3.5x1/4
12	14WF38	24WF84	L4x3-1/2x1/2	12WF40	10WF49	L4x3-1/2x1/2	16B26	10WF60	L6x3.5x1/4
13	12WF31	16WF40	L7x4x3/8	12WF31	12WF36	L7x4x3/8	16B26	10WF39	L6x3.5x1/4
14	12WF40	21WF50	L5x5x7/16	12WF40	12WF40	L5x5x7/16	16B26	10WF49	L6x3.5x1/4
15	14WF43	10WF72	L6x3-1/2x1/2	16WF36	21WF62	L6x3-1/2x1/2	16B31	12WF53	L6x3.5x5/16
16	18WF50	10WF100	L7x4x7/16	18WF45	24WF94	L7x4x7/16	16WF40	12WF72	L6x3.5x5/16

Note: Section sizes obtained from CISC Properties of Shapes, Plates, Bars and Tubes (1965), WF refers to a wide flange shape similar to current W-sections and B refers to a standard American shape similar to current S-sections.

Table 3. Failure criteria based on average axial brace elongation of the 16 buildings

Failure Type	δ_{ult}/L	Failure Type	δ_{ult}/L	Failure Type	δ_{ult}/L
	%		%		%
Net section (Category 1)	0.23	Bolt shear fracture	0.25	Bolt bearing	0.31
Net section (Category 2)	0.29	Block shear rupture	0.31	Inelastic drift limit	2.50*
Net section (Category 3)	0.39				

*Note: Value corresponds to horizontal building drift.

Table 4. Ground motion records (Abbotsford BC)

ID	*Event*	*Magnitude*	*Station*	*Distance* (km)	*Duration* (sec)	*Scale Factor*[*]
	Historical ground motions (McGuire 2004)					
963	Jan. 17, 1994 Northridge	6.7	Castaic, Old Ridge Route	44	9.08	0.6
1005	Jan. 17, 1994 Northridge	6.7	LA - Temple & Hope	37	13.3	1.7
1039	Jan. 17, 1994 Northridge	6.7	Moorpark - Fire Sta	36	14.2	1.3
735	Oct. 18, 1989 Loma Prieta	6.9	APEEL 7 - Pulgas	65	14.7	2.1
776	Oct. 18, 1989 Loma Prieta	6.9	Hollister - South & Pine	51	28.7	1.2
787	Oct. 18, 1989 Loma Prieta	6.9	Palo Alto - SLAC Lab	54	11.6	1.1
796	Oct. 18, 1989 Loma Prieta	6.9	SF-Presidio	99	8.7	1.4
900	June 28, 1992 Landers	7.3	Yermo Fire Station	86	17.6	0.9
1794	Oct. 16, 1999 Hector Mines	7.1	Joshua Tree	54	12.9	1.4
15	July 21, 1952 Kern County	7.4	Taft Lincoln School	46	30.3	2.0
	Simulated ground motions (Atkinson 2009)					
10	West6C1	6.5	-	10	3.3	1.0
34	West6C1	6.5	-	12	4.6	1.0
37	West7C1	7.5	-	26	33.6	1.4
13	West7C2	7.5	-	30	29.4	1.0
1	West7C2	7.5	-	47	35.6	1.6
7	West7C2	7.5	-	49	36.8	2.0
11	West7C2	7.5	-	51	38.2	2.4
16	West7C2	7.5	-	65	34.4	2.0
22	West7C2	7.5	-	70	33.8	2.4
39	West7C2	7.5	-	100	37.4	2.8

*Ground motion records initially scaled to UHS

Table 5. Ground motion records (Montreal QC)

ID	*Event*	*Magnitude*	*Station*	*Distance* (km)	*Duration* (sec)	*Scale Factor*[*]
	Historical ground motions (McGuire 2004)					
CCN090	Jan. 17, 1994 Northridge	6.7	LA-Century City CC North	26	15.6	0.4
WAI290	Jan. 17, 1994 Northridge	6.7	Huntington Beach Waikiki	57	19.8	1.3
HNT000	Jan. 17, 1994 Northridge	6.7	Huntington Beach Lake St	76	30.0	1.6
DEL090	Jan. 17, 1994 Northridge	6.7	Lakewood Del Amo Bvld	59.3	21.0	0.8
H-E01140	Oct 15, 1979 Imperial Valley	6.5	El Centro Array #1	16	14.7	1.0
H-CXO315	Oct 15, 1979 Imperial Valley	6.5	Calexico Fire Station	11	16.8	0.6
MUL279	Oct. 1, 1987 Whittier Narows	6.0	Beverly Hills - 14145 Mulhol	30	17.4	0.9
A-STC090	Oct. 1, 1987 Whittier Narows	6.0	Northridge- 17645 Saticoy St	40	14.3	1.0
IND000	June 28, 1992 Landers	7.3	Indio-Coachella Canal	56	38.3	0.8
HOS180	June 28, 1992 Landers	7.3	San Bernardino-E&Hospitality	80	46.0	0.5
	Simulated ground motions (Atkinson 2009)					
15	East6C1	6.0	-	11	2.4	0.5
1	East6C1	6.0	-	13	1.0	0.5
30	East6C1	6.0	-	14	2.1	0.8
34	East6C1	6.0	-	17	2.0	0.8
32	East7C1	7.0	-	26	7.5	0.8
3	East7C2	7.0	-	42	8.3	1.2
8	East7C2	7.0	-	45	6.4	1.7
5	East7C2	7.0	-	50	8.4	1.7
40	East7C2	7.0	-	94	7.6	2.1
35	East7C2	7.0	-	100	8.8	2.1

*Ground motion records initially scaled to UHS

Table 6. Ground motion records (Halifax NS)

ID	*Event*	*Magnitude*	*Station*	*Distance* (km)	*Duration* (sec)	*Scale Factor*[*]
	Historical ground motions (McGuire 2004)					
CCN090	Jan. 17, 1994 Northridge	6.7	LA-Century City CC North	26	15.6	0.21
WAI290	Jan. 17, 1994 Northridge	6.7	Huntington Beach Waikiki	57	19.8	0.42
HNT000	Jan. 17, 1994 Northridge	6.7	Huntington Beach Lake St	76	30.0	0.65
DEL090	Jan. 17, 1994 Northridge	6.7	Lakewood Del Amo Bvld	59.3	21.0	0.47
H-E01140	Oct 15, 1979 Imperial Valley	6.5	El Centro Array #1	16	14.7	0.45
H-CXO315	Oct 15, 1979 Imperial Valley	6.5	Calexico Fire Station	11	16.8	0.31
MUL279	Oct. 1, 1987 Whittier Narows	6.0	Beverly Hills - 14145 Mulhol	30	17.4	0.50
A-STC090	Oct. 1, 1987 Whittier Narows	6.0	Northridge- 17645 Saticoy St	40	14.3	0.36
IND000	June 28, 1992 Landers	7.3	Indio-Coachella Canal	56	38.3	0.44
HOS180	June 28, 1992 Landers	7.3	San Bernardino-E&Hospitality	80	46.0	0.40
	Simulated ground motions (Atkinson 2009)					
1	East6C2	6.0	-	-	4.2	0.44
3	East6C2	6.0	-	-	4.2	0.70
5	East6C2	6.0	-	-	4.2	0.60
9	East6C2	6.0	-	-	5.5	0.47
15	East6C2	7.0	-	-	4.3	0.67
1	East7C2	7.0	-	-	16.3	0.59
2	East7C2	7.0	-	-	16.3	0.71
3	East7C2	7.0	-	-	16.3	0.64
7	East7C2	7.0	-	-	14.0	0.65
8	East7C2	7.0	-	-	14.0	0.79

*Ground motion records initially scaled to UHS

Table 7. Percentage of buildings meeting acceptable performance levels based on anticipated failure mode

Location	*Failure mode*						
	Net section Cat 1	Net section Cat 2	Net section Cat 3	Bolt shear fracture	Block shear rupture	Bolt bearing	Inelastic drift limit
Abbotsford, BC	0 %	0 %	0 %	0 %	0 %	0 %	88 %
Montreal, QC	13 %	38 %	100 %	13 %	38 %	38 %	100 %
Halifax, NS	94 %	100 %	100 %	100 %	100 %	100 %	100 %*

* None of the Halifax buildings reached the 2.5% inelastic drift limit at an IDA scaling factor of 6.

Table 8. Adjusted collapse margin ratios (ACMR) for buildings in Abbotsford, BC (high seismicity)

Building	*Failure mode*						
	Net section Cat 1	Net section Cat 2	Net section Cat 3	Bolt shear fracture	Block shear rupture	Bolt bearing	Inelastic drift limit
1A	0.60	0.74	0.94	0.68	0.77	0.82	1.86
2A	0.64	0.81	1.06	0.73	0.84	0.90	2.25
3A	0.64	0.84	1.11	0.73	0.88	0.92	2.55
4A	0.65	0.79	1.01	0.68	0.83	0.82	2.40
5A	0.58	0.74	0.96	0.65	0.77	0.80	2.10
6A	0.64	0.79	0.97	0.67	0.82	0.82	2.52
7A	0.64	0.80	1.01	0.69	0.84	0.84	2.83
8A	0.71	0.89	1.13	0.75	0.93	0.92	3.03
9A	0.59	0.73	0.90	0.64	0.76	0.77	1.21
10A	0.62	0.78	1.00	0.66	0.83	0.82	2.79
11A	0.67	0.85	1.07	0.70	0.90	0.88	2.85
12A	0.67	0.82	1.03	0.69	0.88	0.84	3.15
13A	0.68	0.85	1.06	0.72	0.87	0.88	2.99
14A	0.71	0.88	1.11	0.73	0.93	0.89	3.20
15A	1.00	1.17	1.39	1.02	1.23	1.18	3.82
16A	0.69	0.85	1.05	0.67	0.89	0.84	3.34
Avg.	0.67	0.83	1.05	0.71	0.87	0.87	2.68

Table 9. Adjusted collapse margin ratios (ACMR) for buildings in Montreal, QC (moderate seismicity)

Building	*Failure mode*						
	Net section Cat 1	Net section Cat 2	Net section Cat 3	Bolt shear fracture	Block shear rupture	Bolt bearing	Inelastic drift limit
1M	1.15	1.48	1.96	1.33	1.54	1.67	5.58
2M	1.21	1.72	2.22	1.48	1.76	1.87	5.74
3M	1.26	1.64	2.28	1.45	1.72	1.79	6.53
4M	1.38	1.77	2.34	1.49	1.86	1.85	6.30
5M	1.15	1.51	2.01	1.29	1.56	1.61	5.35
6M	1.23	1.59	2.06	1.31	1.68	1.67	6.42
7M	1.35	1.77	2.42	1.47	1.89	1.89	7.32
8M	1.76	2.21	2.98	1.89	2.33	2.32	7.97
9M	1.18	1.55	2.03	1.29	1.64	1.65	6.34
10M	1.40	1.84	2.44	1.50	1.96	1.95	7.21
11M	1.75	2.29	2.98	1.86	2.44	2.39	7.94
12M	2.00	2.39	3.09	2.04	2.58	2.45	9.40
13M	1.42	1.82	2.44	1.51	1.87	1.90	7.90
14M	1.80	2.27	2.93	1.86	2.41	2.31	9.04
15M	1.85	2.30	2.85	1.90	2.46	2.32	8.41
16M	2.06	2.57	3.17	1.99	2.70	2.53	9.31
Avg.	1.50	1.92	2.51	1.60	2.02	2.01	7.30

Table 10. Adjusted collapse margin ratios (ACMR) for buildings in Halifax, NS (low seismicity)

Building	*Failure mode*						
	Net section Cat 1	Net section Cat 2	Net section Cat 3	Bolt shear fracture	Block shear rupture	Bolt bearing	Inelastic drift limit
1H	2.41	3.12	4.25	2.92	3.32	3.60	-
2H	2.29	3.03	4.18	2.73	3.16	3.47	-
3H	2.40	3.05	3.92	2.75	3.14	3.25	-
4H	2.38	3.29	3.96	2.60	3.44	3.43	-
5H	1.98	2.55	3.32	2.21	2.76	2.85	-
6H	1.93	2.55	3.27	2.08	2.77	2.75	-
7H	2.17	2.69	3.52	2.25	2.88	2.88	-
8H	3.16	3.83	5.12	3.35	3.97	3.95	-
9H	2.80	3.57	4.40	3.03	3.72	3.74	-
10H	2.54	3.27	4.08	2.73	3.42	3.41	-
11H	2.41	3.17	3.92	2.56	3.38	3.30	-
12H	2.23	2.83	3.56	2.30	3.05	2.86	-
13H	2.56	3.03	3.60	2.67	3.13	3.11	-
14H	2.34	2.82	3.28	2.43	2.93	2.86	-
15H	2.88	3.49	4.29	2.93	3.65	3.50	-
16H	2.22	2.92	3.63	2.20	3.09	2.82	-
Avg.	2.42	3.08	3.89	2.61	3.24	3.24	-

Figure 1. Typical structural framework of single-storey CBF building located in Canada.

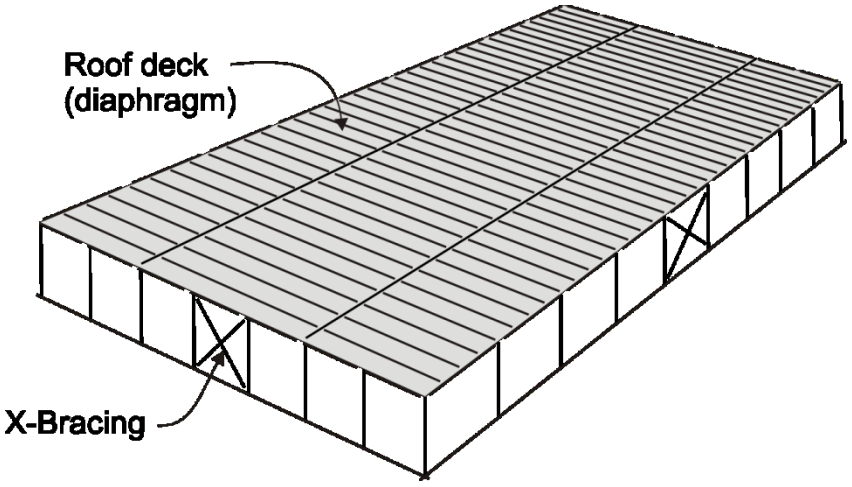

Figure 2. Conceptual approach to seismic design of lateral force resisting system: a) 1965 NBCC elastic lateral design; b) Current inelastic capacity based design.

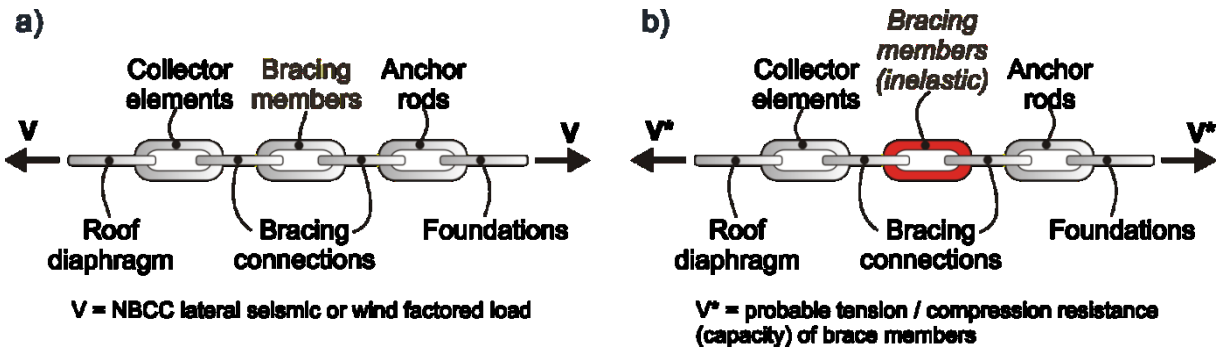

Figure 3. Net-section fracture of 1965 single-angle braces: a) Brittle fracture of specimen 3BSB (Net-section Category 1); b) Increased deformations at fracture showing more ductile failure of specimen 3CS (Net-section Category 2); c) Additional deformations at fracture surface of specimen 3AS (bolt removed post-test) (Net-section Category 3) (Caruso-Juliano 2012).

a) b) c)

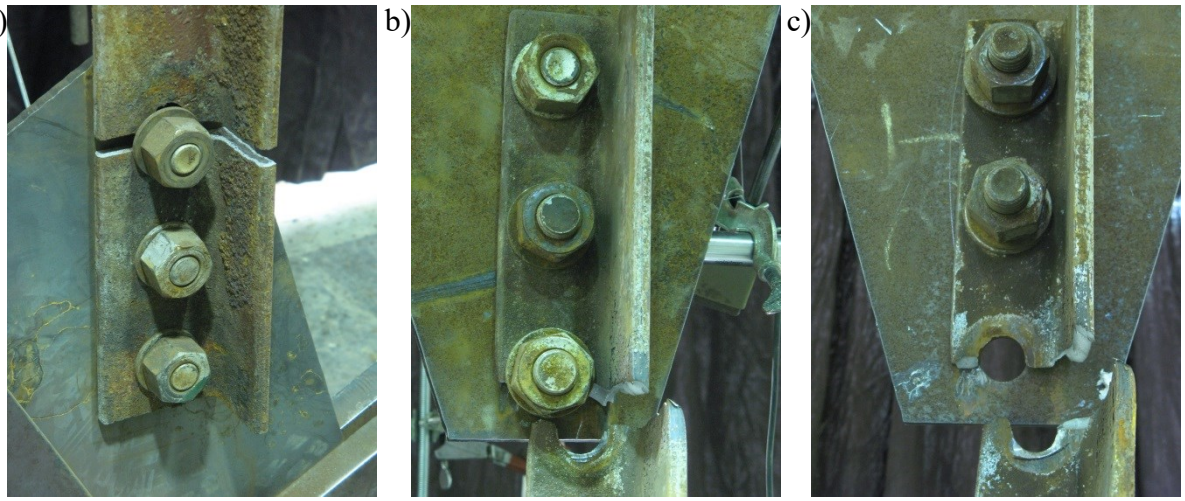

Figure 4. a) Numerical building model accounting for inelastic brace response and elastic flexible roof diaphragm response and b) Details of bracing bent model.

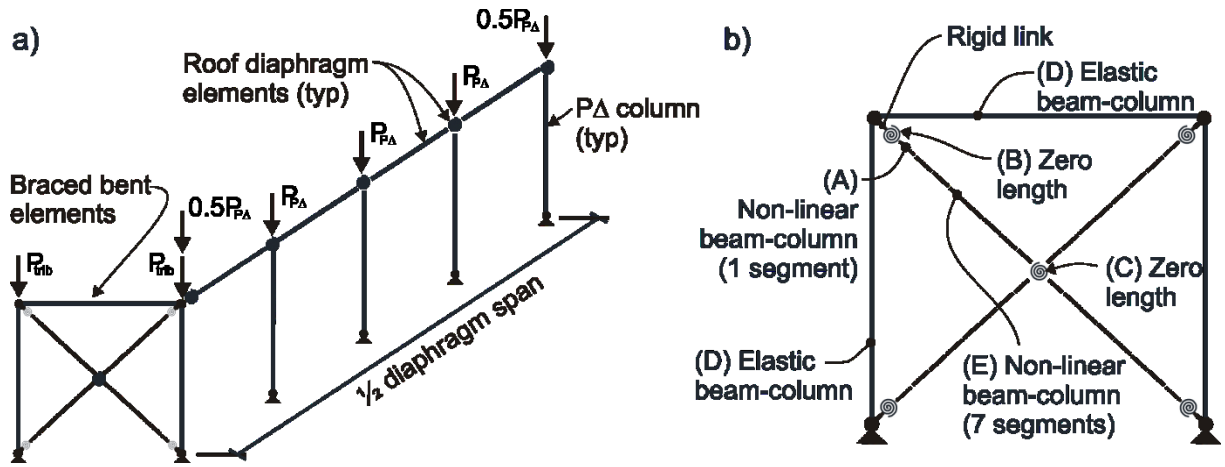

Figure 5. a) Single angle brace resistance vs. deformation hysteretic Steel02 element response and b) Fibre element discretization of brace member.

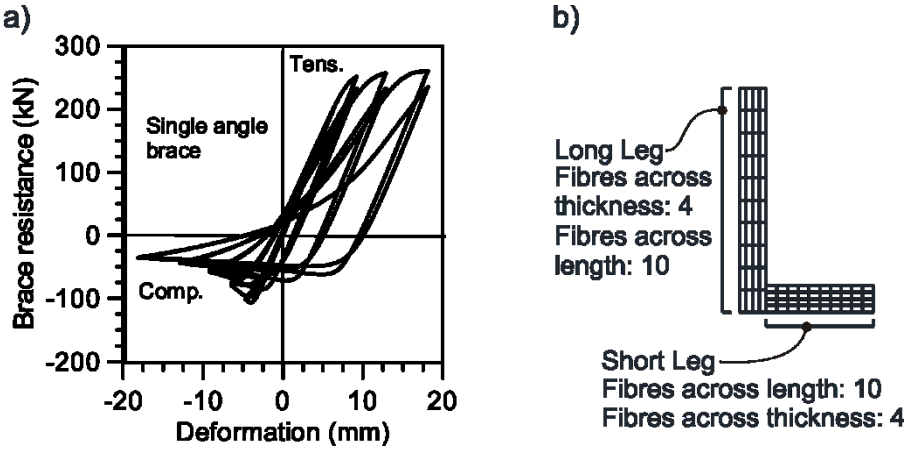

Figure 6. Comparison of numerical bracing bent model and measured response; a) Numerical model of test bracing bent, b) Test bracing bent, c) Hysteretic force vs. displacement response, d) Dissipated energy vs. cumulative displacement.

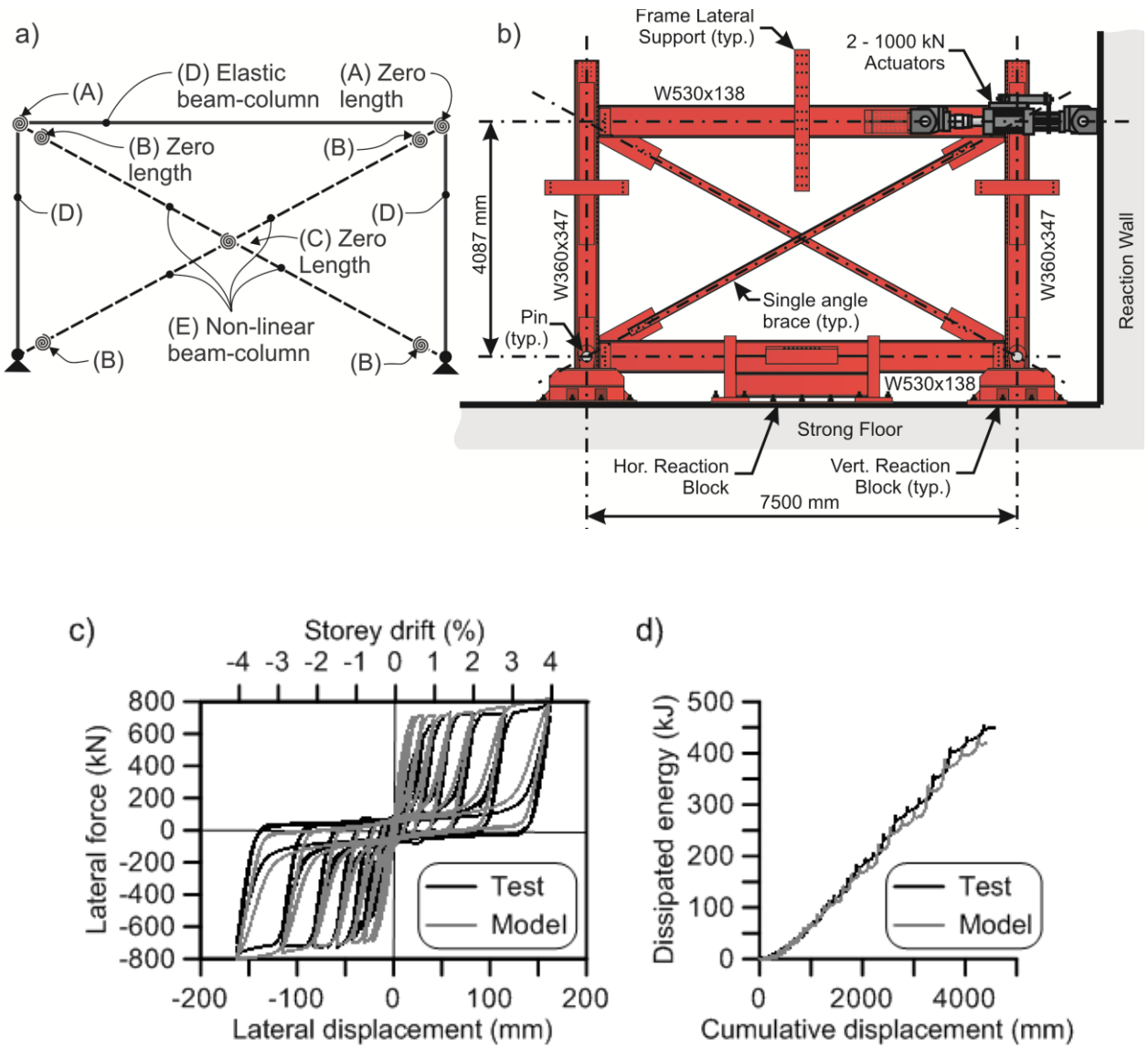

Figure 7. Scaled response spectra of 20 ground motions vs. 2010 NBCC design uniform hazard spectrum (UHS) for: a) Halifax, NS, b) Montreal, QC, and c) Abbotsford, BC.

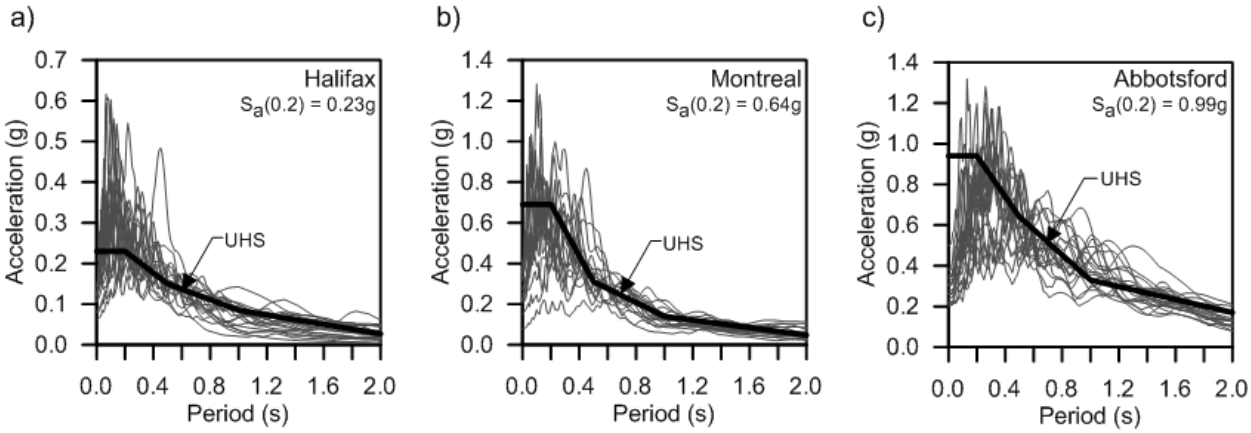

Figure 8. Example time history for Abbotsford building; a) ground motion scaled to UHS and b) diaphragm shear force and resistance calculated using SDI method (Luttrell 2004)

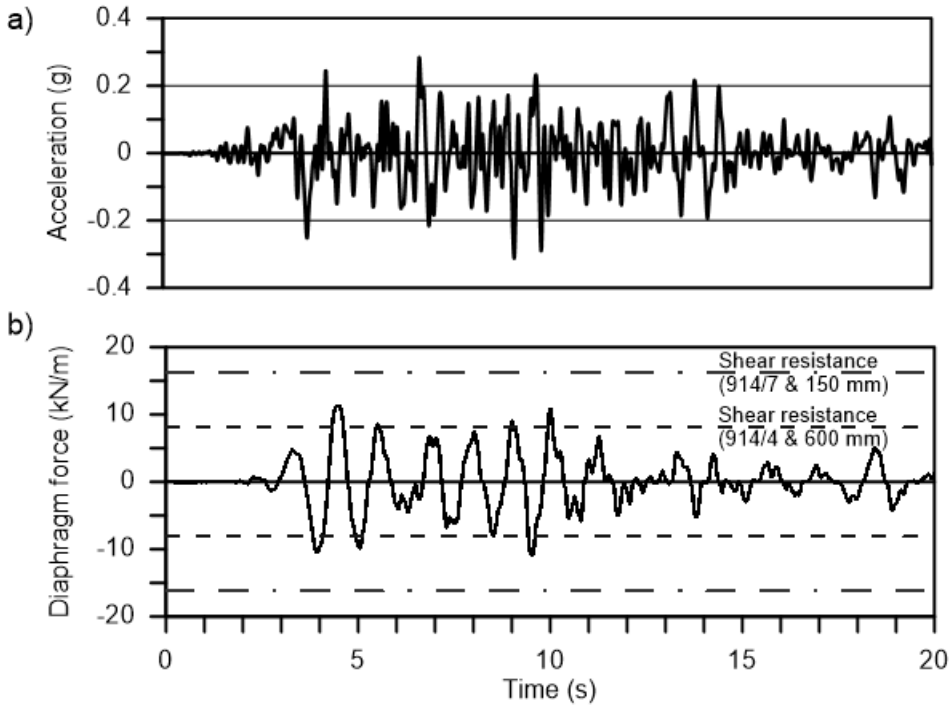

Figure 9. Example fragility curves and uncertainty adjusted fragility curves for building 8: a) Abbotsford, BC, b) Montreal, QC and c) Halifax, NS.